ISSN 1063-7710, Acoustical Physics, 2023, Vol. 69, No. 6, pp. 782–787. © Pleiades Publishing, Ltd., 2023.
Russian Text © The Author(s), 2023, published in Akusticheskii Zhurnal, 2023, Vol. 69, No. 6, pp. 695–701.

PHYSICAL ACOUSTICS

# Reduction of the Spin–Phonon Coupling of Quadrupole Nuclei in NaF Crystals under Magnetic Saturation

**V. M. Mikushev[a], *, A. M. Rochev[a], and E. V. Charnaya[a], ****

[a] *St. Petersburg State University, St. Petersburg, 198504 Russia*

**e-mail: v.mikushev@spbu.ru*

***e-mail: charnaya@spbu.ru*

Received April 27, 2023; revised May 22, 2023; accepted June 22, 2023

**Abstract**—The rate of nuclear spin-lattice relaxation is determined by the efficiency of interaction between thermal phonons and nuclear spins. The results on reducing the efficiency of spin–phonon coupling by suppressing the contribution from paramagnetic centers to quadrupole nucleus relaxation are presented. The suppression has been performed by continuous magnetic action at the Larmor frequency. It is shown that, as in the presence of an acoustic field, the rate of spin-lattice relaxation of $^{23}$Na nuclei in a sodium fluoride crystal at magnetic saturation of the NMR signal does not change in the region of a negative average spin temperature. In the region of positive spin temperature, the rate of relaxation of $^{23}$Na spins significantly decreases and nuclear magnetization recovery with time is described by the sum of two exponentials. The contribution from nuclear spins with a lower efficiency of spin–phonon coupling, corresponding to the exponential with a long relaxation time, increases with increasing saturating field intensity. It is demonstrated that the efficiency of spin–phonon coupling for $^{19}$F nuclei, which do not have the quadrupole moment, does not change under the saturation conditions. The results obtained can be used for analyzing the structure of real crystals.

**Keywords:** magnetic quantum acoustics, nuclear spin–phonon coupling, acoustic and magnetic saturation of the NMR line, spin-lattice relaxation, paramagnetic centers

**DOI:** 10.1134/S1063771023601103

## INTRODUCTION

The efficiency of spin–phonon coupling determines the rate of nuclear spin-lattice relaxation (SLR), characterized by the time $T_1^{\Sigma}$ measured by nuclear magnetic resonance (NMR) methods [1]. For nuclei in real dielectric crystals, the total SLR rate is

$$(T_1^{\Sigma})^{-1} = (T_1^{\text{lat}})^{-1} + (T_1^{\text{imp}})^{-1}, \quad (1)$$

where the term $(T_1^{\text{lat}})^{-1}$ is determined by spin–phonon coupling in crystals with an ideal lattice and the "impurity" contribution $(T_1^{\text{imp}})^{-1}$ is caused by the participation of paramagnetic defects and impurities. For nuclei with electrical quadrupole moment, the "lattice" contribution is due to dynamic electric field gradients induced by thermal phonons [2]. The lattice mechanism of relaxation of quadrupole nuclei is dominant in fairly pure samples; however, the role of impurity relaxation increases in doped crystals, especially at temperatures below room temperature [3, 4]. At the same time, relaxation of nuclei with spin ½ is determined almost completely by the addend in Eq. (1). The efficiency of the impurity mechanism of nuclear SLR and its significant contribution to the $T_1^{\Sigma}$ value even at a low concentration of paramagnetic centers in the crystal bulk (e.g., in the presence of unintentional impurities in specially purified samples) are due to the strong coupling of paramagnetic centers with lattice vibrations and with nearest nuclear spins and to the participation of spin diffusion equalizing the nuclear magnetization in the sample bulk [3].

Two methods are applied in magnetic quantum acoustics to observe nuclear acoustic resonance (NAR), at which transitions between nuclear Zeeman levels are induced by either a traveling acoustic wave or a diffusively scattered resonant-frequency acoustic field [5, 6]. Resonance absorption of an acoustic energy by the nuclear spin system is directly recorded in the "direct" NAR method. In the method of acoustic saturation of NMR signals, a decrease in the difference between spin level populations is investigated proceeding from the change in the NMR signal intensity, which can be considered as a consequence of the increase in the average spin temperature in a nuclear ensemble [7]. The NMR saturation method is much more popular in view of high sensitivity and universality. Investigations of acoustic saturation of an NMR signal of quadrupole nuclei showed that the saturation process is similar to a reverse process of nuclear SLR. In ideal crystals, the saturation is due to acoustic modulation of crystalline electric fields. The presence of

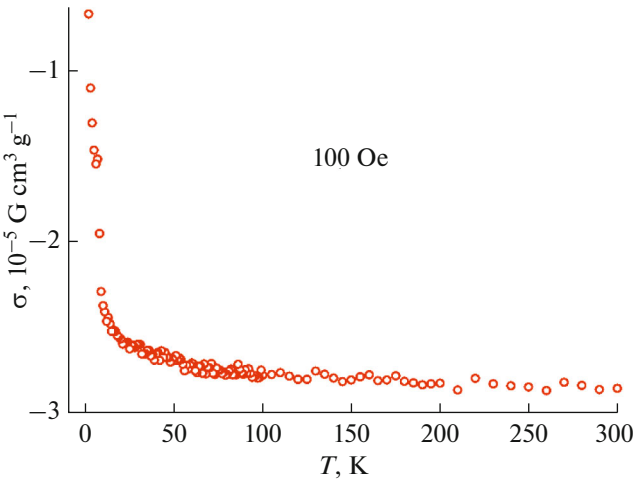


**Fig. 1.** Temperature dependence of specific magnetization σ of sodium fluoride crystal upon cooling in magnetic field of 100 Oe.

paramagnetic centers of a different nature induces an additional channel of acoustic saturation owing to the local overheating of the spin system of nearest (to these centers) nuclei and spin diffusion [8–10]. A local increase in the spin nuclear temperature near a certain paramagnetic center suppresses the contribution of this center to the impurity relaxation, which reduces the rate of the total SLR $(T_1^{\Sigma})^{-1}$. Thus, the use of acoustic saturation of the NMR signal made it possible to separate the mechanisms of SLR of quadrupole nuclei and measure the times $(T_1^{\text{lat}})^{-1}$ and $(T_1^{\text{imp}})^{-1}$ in some materials by observing the nuclear magnetization recovery to the equilibrium value under the saturation conditions [11–13]. It should be emphasized that investigation of the mechanisms of spin–phonon coupling in different materials is an issue of fundamental importance for many practical applications [6, 14]. The aim of this study is to analyze the possibility of separation of the lattice and impurity contributions to the spin–phonon coupling under magnetic saturation of the NMR line for quadrupole sodium nuclei in a NaF crystal and compare it with the case of fluorine nuclei without the quadrupole moment.

## EXPERIMENTAL

Samples were cut from a sodium fluoride (NaF) single crystal along the fourfold symmetry axis. The composition of the crystal was analyzed for the presence of impurities in the bulk, incorporated into a lattice during growth. Quantitative elemental analysis of a specimen taken from the crystal bulk was carried out on an ICPE-9000 optical inductively coupled plasma emission spectrometer (Shimadzu). The analysis revealed the following contents of impurity atoms in the NaF crystal under study: 310 for Ca, 10.5 for Mg, 7.9 for Fe, 6.1 for Zn, and 3.1 mg/kg for Sr.

Investigation of the NaF sample using an MPMS SQUID VSM magnetometer (Quantum Design) revealed weak paramagnetism due to unintentional paramagnetic centers against the background of diamagnetic magnetization (Fig. 1).

NMR measurements were performed on a Bruker Avance III 400 pulsed spectrometer, optimized for studying solid samples, at temperatures of 296 and 155 K. Magnetization recovery of $^{23}$Na nuclei after inversion by 180° pulse was observed under an additional resonant magnetic saturating impact.

Nuclear magnetization under continuous saturation was characterized by the saturation factor $Z^{st} = A^{st}/A_0$, where $A^{st}$ and $A_0$ are the integral intensities of the $^{23}$Na NMR lines in the presence and absence of the additional action, respectively [15–17]. To measure the relaxation rate under the saturation conditions, we developed a pulse sequence, the schematic of which is shown in Fig. 2a. The rf pulse $P_1$ with the Larmor filling frequency and width $\Delta t$ no less than $10T_1^{\Sigma}$ was applied before the 180° pulse. The intensity of the pulse $P_1$ varies in different measurements to provide continuous saturation of different extent. In the interval between the 180° and 90° pulses, the rf pulse $P_2$ with the same intensity as $P_1$ was applied. The width of the pulse $P_2$ depended on the delay time between the 180° and 90° pulses, set to measure the nuclear magnetization recovery rate. After the 90° pulse, a free-precession signal is recorded, the Fourier transformation of which yields the NMR line. The dependence of the integral intensity of the NMR line $A$ on the delay time $t$ between the inverting and probe pulses makes it possible to plot the curve of nuclear magnetization recovery $Z(t) = A(t)/A_0$ to the stationary value (as shown in Fig. 2b) and calculate the recovery time τ.

In the case of the presence of paramagnetic centers leading to inhomogeneity of the nuclear magnetization, the volume-averaged spin temperature $\langle T_I \rangle$ is introduced [7]. Parameter $Z$ can be expressed in this case in terms of the ratio of the inverse spin temperature $\langle \alpha_I \rangle \equiv \dfrac{\hbar}{k_B \langle T_I \rangle}$ to the inverse lattice temperature $\alpha_l \equiv \dfrac{\hbar}{k_B T_l}$ ($T_l$ is the lattice temperature): $Z = \dfrac{\langle \alpha_I \rangle}{\alpha_l}$. Thus, the nuclear magnetization recovery occurs in the range of negative spin temperatures in the initial stage (up to the instant $t_0$) (Fig. 2b) and in the range of positive spin temperatures at $t > t_0$. When the impurity contribution to the SLR is not suppressed, for each value of the saturation factor $Z^{st}$, the total relaxation time $T_1^{\Sigma}$ is related to the time τ of nuclear magnetiza-

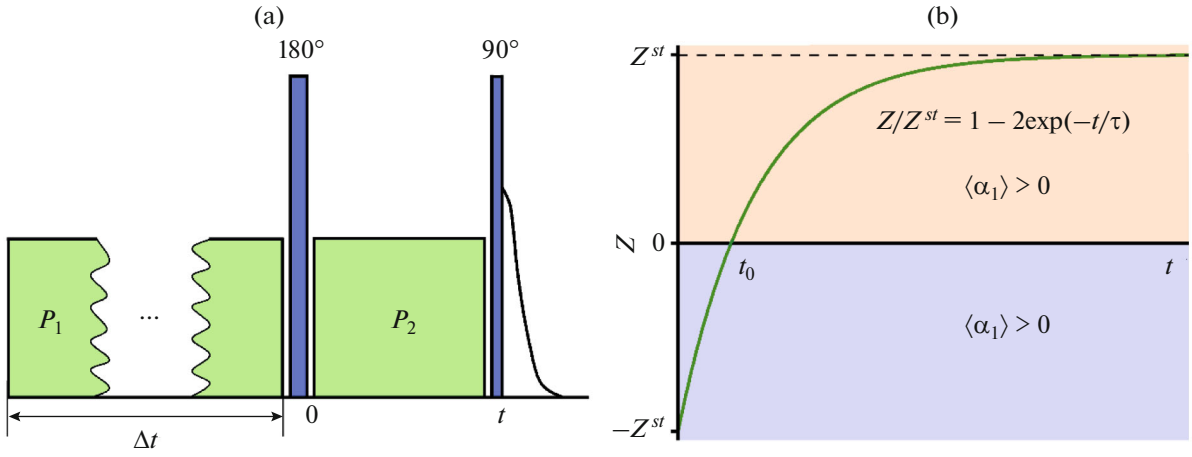


**Fig. 2.** (a) Pulse sequence for observing nuclear magnetization recovery under magnetic saturation of NMR line. Additional resonance rf pulses $P_1$ and $P_2$ provide continuous magnetic saturation with factor $Z^{st}$. (b) Nuclear magnetization recovery after 180° pulse to $Z^{st}$: $\tau$ is recovery time, $t_0$ is time at which nuclear magnetization is zero, and $\langle\alpha_I\rangle$ is volume-averaged inverse spin temperature.

tion recovery under continuous saturation (Fig. 2b) by the expression

$$T_1^{\Sigma} = \tau / Z^{st}. \quad (2)$$

Relation (2) is a consequence of the known equation for the change in the inverse spin temperature under resonance excitation and SLR [7]:

$$\frac{\partial\langle\alpha_I\rangle}{\partial t} = \frac{\alpha_I - \langle\alpha_I\rangle}{T_1^{\Sigma}} - W\langle\alpha_I\rangle = \frac{\alpha_I}{T_1^{\Sigma}} - \frac{\langle\alpha_I\rangle}{Z^{st}T_1^{\Sigma}}, \quad (3)$$

where $W$ is the probability of induced transitions and $Z^{st} = 1/(1 + WT_1^{\Sigma})$. The solution to Eq. (3) demonstrates the exponential recovery of the inverse spin temperature to the equilibrium value with time $\tau$ obeying relation (2).

## RESULTS AND DISCUSSION

Recovery of $^{23}$Na nuclear magnetization after inversion by the 180° pulse was measured at temperatures of 296 and 155 K in the ranges of magnetic-saturation factor from 1 to 0.07 and from 1 to 0.06, respectively. The relaxation times $T_1^{\Sigma}$ obtained in the absence of saturation ($Z^{st} = 1$) were 12.4 and 54.6 s at 296 and 155 K, respectively. It was shown that the behavior of the recovery curves $Z(t)$ at both temperatures in the initial stage in the range of negative spin temperatures was exponential and characterized by the times $\tau_1 = T_1^{\Sigma}Z^{st}$ in accordance with expression (2) at all values of the saturation factor. With allowance for the incomplete inversion of the nuclear magnetization after the inverting pulse, the curves $Z(t)$ were described by the expression

$$Z(t) = Z^{st}\left[1 - b\exp\left(-t/\tau_1\right)\right], \quad (4)$$

where $b$ is a numerical coefficient ($1 < b < 2$). Thus, the additional magnetic saturation did not affect the efficiency of spin–phonon coupling of sodium nuclei in the region of negative average spin temperatures at any saturation level.

The single-exponential process of nuclear magnetization recovery with the times $\tau_1 = T_1^{\Sigma}Z^{st}$ was also observed in the region of positive average spin temperatures but at limited saturation factors $Z^{st} > 0.4$ and $Z^{st} > 0.7$ for the temperatures of 296 and 155 K, respectively. At stronger saturation, the dependence $Z(t)$ in the range $\langle\alpha_I\rangle > 0$ ($t > t_0$) was described by the sum of two exponentials with the magnetization recovery times $\tau_1$ and $\tau_2 > \tau_1$

$$Z(t) = Z^{st}\left\{1 - b\left[\rho\exp\left(-t/\tau_1\right) + (1-\rho)\exp\left(-t/\tau_2\right)\right]\right\}, \quad (5)$$

where $\rho$ is the weighting coefficient characterizing the relative contribution from the lattice relaxation mechanism. The occurrence of the second exponential with a long time of nuclear magnetization recovery demonstrates a decrease in the efficiency of spin–phonon coupling for a part of nuclei and corresponds to a decrease in the $^{23}$Na SLR rate. As an example, Fig. 3 shows the behavior of nuclear magnetization recovery at 296 K for the continuous saturation factor $Z^{st} = 0.11$. It should be noted that the possibility of calculating the nuclear magnetization recovery curve as the

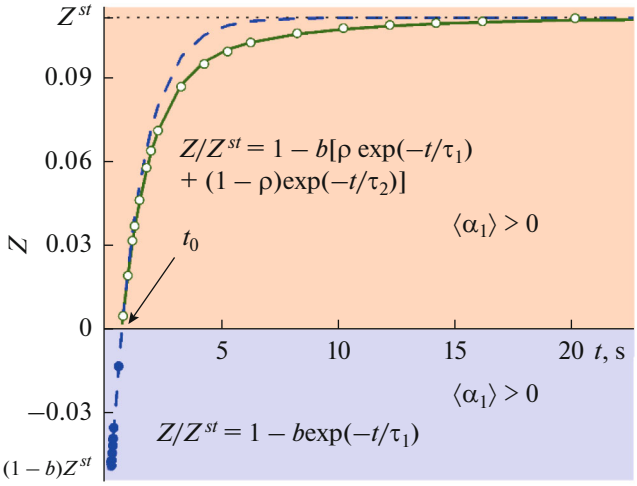


**Fig. 3.** Nuclear magnetization recovery after 180° pulse at continuous saturation $Z^{st} = 0.11$ for $T = 296$ K. Dashed and solid lines plotted using formula (5) with $\rho = 1$ and $\rho < 1$ at $t > t_0$, respectively.

sum of two exponentials at sufficiently strong saturation is due to high measurement accuracy, which was unattainable in earlier studies on suppression of the impurity relaxation mechanism.

Expression (5) can be extended to the region of negative spin temperatures, assuming that $\rho = 1$ at $t < t_0$.

Figure 4 shows values of the weighting coefficient $\rho$ for the "fast" SLR with the recovery time $\tau_1$ calculated from (5) using the experimental dependences of $^{23}$Na nuclear magnetization recovery for different continuous magnetic saturation factors $Z^{st}$ at two temperatures.

Figure 5 shows the dependence of the nuclear magnetization recovery times $\tau_1$ and $\tau_2$ on the continuous saturation factor $Z^{st}$. The linear dependences between time $\tau_1$ and factor $Z^{st}$ at two temperatures are in agreement with Eq. (2) and the values of times $T_1^{\Sigma}$ measured in the absence of magnetic saturation. A contribution from the slower relaxation process, which is characterized by the recovery times $\tau_2 > \tau_1$, occurs at the threshold values of the continuous saturation factor at times $t > t_0$. A fraction of this contribution increases with decreasing saturation factor.

Single-exponential relaxation in the region of negative spin temperatures at any intensity of the additional resonance field saturating the nuclear spin system indicates that the impurity mechanism is not suppressed. Within the thermodynamic approach [7] to the description of the behavior of the sodium nuclear spin system, the impurity contribution to the spin–phonon coupling is efficient if the local inverse spin temperature $\alpha_{loc}$ is closer to the inverse lattice temperature $\alpha_l$ than the volume-averaged inverse spin temperature $\langle\alpha_I\rangle$ [18]. In the region of negative spin temperatures, the condition

$$|\alpha_{loc} - \alpha_l| < |\langle\alpha_I\rangle - \alpha_l| \quad (6)$$

is always satisfied, even in the case of local overheating of the nuclear spin system near paramagnetic centers to values of $\alpha_{loc} \approx 0$.

In the range $t > t_0$, at $\langle\alpha_I\rangle > 0$, fairly strong additional continuous saturation leads to local overheating of the spin system near certain paramagnetic centers (to a decrease in the local inverse spin temperature)

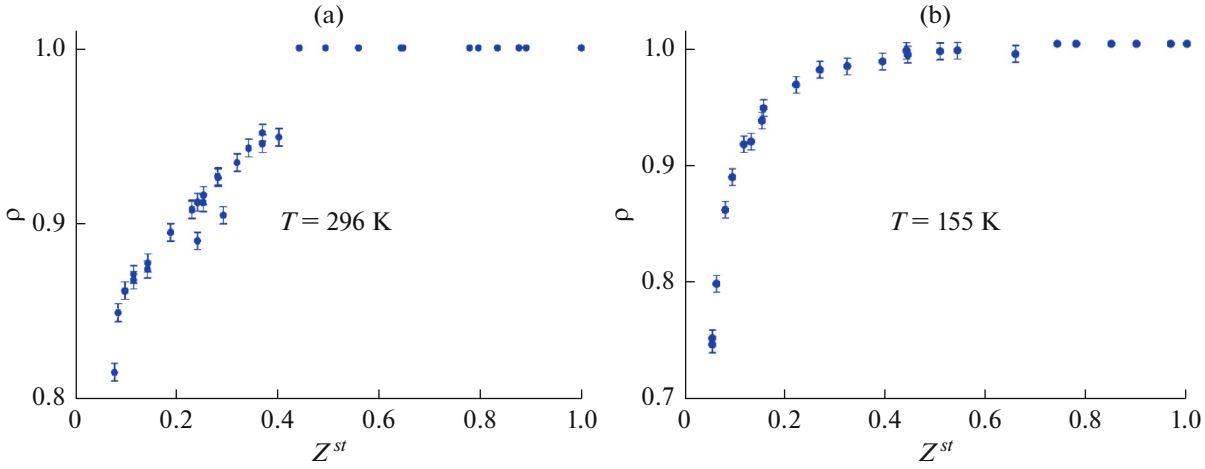


**Fig. 4.** Weighting coefficient $\rho$ calculated from (5) using experimental curves of $^{23}$Na nuclear magnetization recovery for different $Z^{st}$ at temperatures of (a) 296 and (b) 155 K.

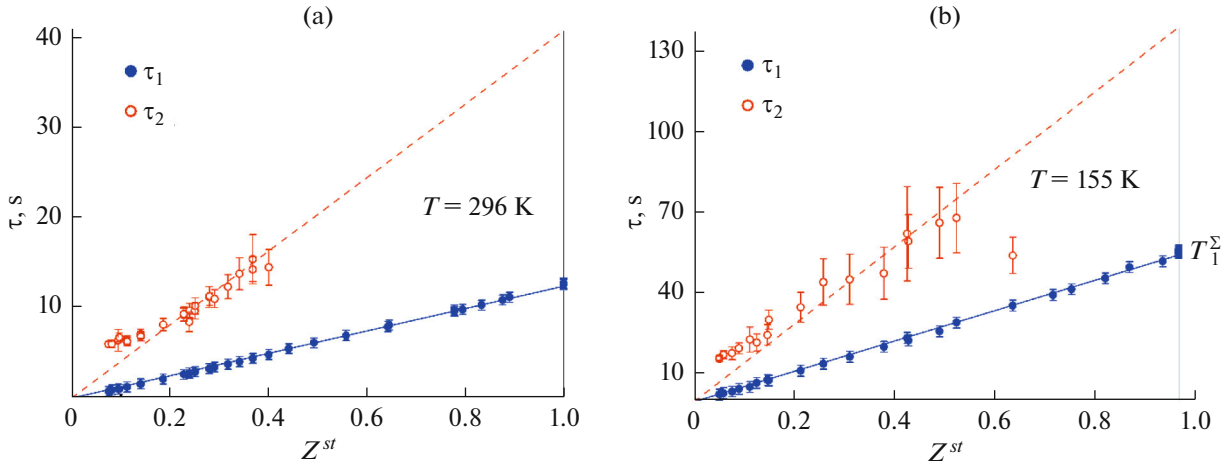


**Fig. 5.** Nuclear magnetization recovery times $\tau_1$ and $\tau_2$ for $^{23}$Na as function of continuous magnetic saturation factor $Z^{st}$.

and to inversion of inequality (6). Thus, the impurity relaxation is suppressed. Since the suppression occurs at different continuous saturation levels for different paramagnetic centers in the presence of unintentional impurities and point defects in the crystal, one might expect a gradual increase in the slow relaxation contribution with an increase in $Z^{st}$ (as was observed experimentally). The times $\tau_2$ correspond to the time of nuclear magnetization recovery only due to the lattice mechanism of spin–phonon coupling. Note that the theoretical model of overheating of the nuclear spin system under continuous magnetic saturation was proposed in [19].

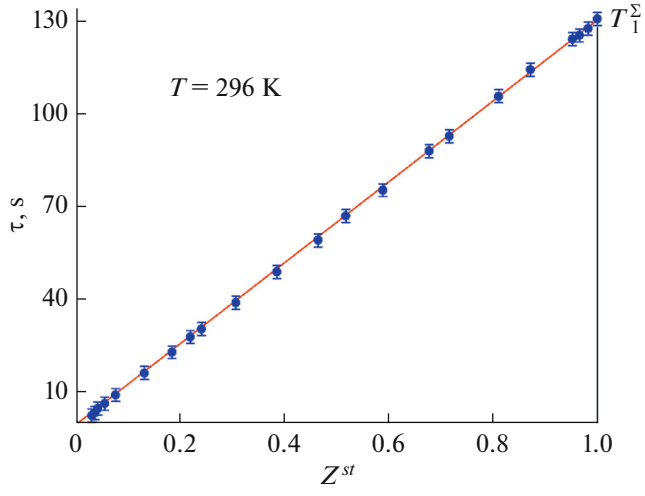


**Fig. 6.** Magnetization recovery time $\tau$ for $^{19}$F nuclei as function of continuous magnetic saturation factor $Z^{st}$ at temperature of 296 K.

Figure 5 shows that the dependence of $\tau_2$ on the continuous saturation factor is close to linear (as well as the dependence for $\tau_1$). The straight lines plotted using the calculated $\tau_2$ values and passing through the origin should yield at $Z^{st} = 1$ (by analogy with Eq. (2)) the times of SLR due to the lattice mechanism of spin–phonon coupling: $T_1^{lat} \simeq 40$ s at 296 K and $T_1^{lat} \simeq 140$ s at 155 K. The estimates agree with the temperature dependences of the time of spin-lattice relaxation in ideal crystals due to two-phonon Raman processes [4, 20].

We also measured the nuclear magnetization recovery under continuous magnetic saturation for $^{19}$F nuclei in the same NaF crystal. Nuclei of $^{19}$F are characterized by spin 1/2 and do not have quadrupole electrical moment. For dipole nuclei, the main contribution to the SLR is from relaxation due to paramagnetic centers and spin diffusion, whereas the lattice contribution can be neglected [3, 21]. In addition, the saturation for nuclei without quadrupole moment may be implemented without participation of paramagnetic centers. Figure 6 shows the dependence of the nuclear magnetization recovery time $\tau$ on the saturation factor at room temperature. As can be seen, at any $Z^{st}$ values, the process of nuclear magnetization recovery to the stationary value is single exponential (4) with times $\tau$ corresponding to $T_1^{\Sigma} = T_1^{imp} = 131$ s. The result obtained confirms that there is no effect of impurity relaxation suppression for $^{19}$F nuclei.

## CONCLUSIONS

A method for suppressing the contribution from paramagnetic centers to the spin–phonon coupling of $^{23}$Na nuclei with a quadrupole electrical moment under magnetic saturation of the nuclear spin system was realized. It was found that the efficiency of the

spin–phonon coupling of nuclei does not change at negative volume-averaged spin temperatures for any continuous magnetic saturation factor (as in the case of acoustic saturation). In the region of positive spin temperatures, the $^{23}$Na SLR rate decreases with an increase in the stationary saturation $Z^{st}$ to certain values, which is accompanied by suppression of impurity relaxation for a part of the nuclear spin system. The times of the lattice contribution to relaxation at temperatures of 296 and 155 K are estimated from the dependence of the nuclear magnetization recovery time on the saturation factor for this part of nuclei. The proposed technique of separating the impurity and lattice contributions to relaxation under magnetic saturation provides fundamental possibility of studying the impurity composition of dielectric crystals using standard NMR equipment.

## ACKNOWLEDGMENTS

The measurements were carried out with equipment of the Resource Center for Diagnostics of Functional Materials for Medicine, Pharmacology, and Nanoelectronics of St. Petersburg State University Research Park. The compositions and paramagnetic impurity concentrations in the samples were determined at the Chemical Analysis and Materials Research Center and Center for Physical Methods of Surface Investigation of St. Petersburg State University Research Park. Liquid nitrogen was supplied by the Cryogenic Department of St. Petersburg State University Research Park.

## FUNDING

The study was supported by ongoing institutional funding. No additional grants to carry out or direct this particular research were obtained.

## CONFLICT OF INTEREST

The authors of this work declare that they have no conflicts of interest.

## REFERENCES

1. A. Abragam and M. Goldman, *Nuclear Magnetism: Order and Disorder* (Claredon Press, Oxford, 1982; Mir, Moscow, 1984).
2. V. M. Mikushev and E. V. Charnaya, *Nuclear Magnetic Resonance in Solids* (St. Petersburg State Univ., St. Petersburg, 1995) [in Russian].
3. G. R. Khutsishvili, Sov. Phys. Usp. **8** (5), 743 (1965).
4. A. Bakhramov, A. L. Stolypko, E. V. Charnaya, and V. A. Shutilov, Sov. Phys. Solid State **28** (3), 470 (1986).
5. A. R. Kessel', *Nuclear Acoustic Resonance* (Nauka, Moscow, 1969) [in Russian].
6. V. A. Golenishchev-Kutuzov, V. V. Samartsev, N. K. Solovarov, and B. M. Khabibulin, *Magnetic Quantum Acoustics* (Nauka, Moscow, 1977) [in Russian].
7. M. Goldman, *Spin Temperature and Nuclear Magnetic Resonance in Solids* (Claredon Press, Oxford, 1970; Mir, Moscow, 1972).
8. A. A. Kuleshov, V. M. Mikushev, A. L. Stolypko, E. V. Charnaya, and V. A. Shutilov, Sov. Phys. Solid State **28** (11), 1837 (1986).
9. A. A. Kuleshov, V. M. Mikushev, A. L. Stolypko, E. V. Charnaya, and V. A. Shutilov, Sov. Phys. Acoust. **32** (6), 523 (1986).
10. A. A. Kuleshov, V. M. Mikushev, A. L. Stolypko, E. V. Charnaya, and V. A. Shutilov, Sov. Phys. Acoust. **35** (3), 276 (1989).
11. P. Yu. Efitsenko, V. M. Mikushev, and E. V. Charnaya, JETP Lett. **54** (10), 587 (1991).
12. P. Yu. Efitsenko, I. O. Mavlonazarov, V. M. Mikushev, and E. V. Charnaya, Sov. Phys. Solid State **34** (6), 933 (1992).
13. I. O. Mavlonazarov and V. M. Mikushev, Sov. Phys. Solid State **34** (7), 1206 (1992).
14. V. S. Vlasov, A. V. Golov, L. N. Kotov, V. I. Shcheglov, A. M. Lomonosov, and V. V. Temnov, Acoust. Phys. **68** (1), 18 (2022).
15. I. O. Mavlonazarov, V. M. Mikushev, and E. V. Charnaya, JETP Lett. **56** (1), 13 (1992).
16. V. M. Mikushev and E. V. Charnaya, Acoust. Phys. **40** (1), 154 (1994).
17. A. Chandul, E. V. Charnaya, A. A. Kuleshov, V. M. Mikushev, and A. M. Ulyashev, J. Magn. Reson. **135** (1), 113 (1998).
18. V. M. Mikushev, E. V. Charnaya, M. K. Lee, and L.-J. Chang, Results Phys. **12**, 1202 (2019). https://doi.org/10.1016/j.rinp.2019.01.008
19. E. V. Charnaya, V. M. Mikushev, and E. S. Shabanova, J. Phys.: Condens. Matter **6** (37), 7581 (1994). https://doi.org/10.1088/0953-8984/6/37/012
20. V. M. Mikushev, A. A. Ulyashev, E. V. Charnaya, and A. Chandoul, Phys. Solid State **44** (6), 1044 (2002). https://doi.org/10.1134/1.1485005
21. G. A. Persyn and A. W. Nolle, Phys. Rev. **140** (5A), A1610 (1965). https://doi.org/10.1103/PhysRev.140.A1610

*Translated by A. Sin'kov*